Article ID: 1000-7032(2024)07-1173-08

High-performance p-NiO/i-$BaTiO_3$/n-ITO Self-driven UV Photodetectors Controlled by Ferroelectric Effect

HONG Hanzhen[1,2], LIU Kewei[1,2*], YANG Jialin[1], CHEN Xing[1,2], ZHU Yongxue[1], CHENG Zhen[1], LI Binghui[1], LIU Lei[1,2], SHEN Dezhen[1,2]

(1. *State Key Laboratory of Luminescence and Applications, Changchun Institute of Optics, Fine Mechanics and Physics, Chinese Academy of Sciences, Changchun* 130033, *China*;
2. *Center of Materials Science and Optoelectronics Engineering, University of Chinese Academy of Science, Beijing* 100049, *China*)
* *Corresponding Author, E-mail: liukw@ciomp. ac. cn*

Abstract: In recent years, self-driven ultraviolet (UV) photodetectors have become a central focus in both military and civilian fields as they can operate without any external power supply. As a wide bandgap ferroelectric material, Barium titanate ($BaTiO_3$, BTO) possesses good ferroelectric, piezoelectric, and pyroelectric properties, which could generate intrinsic spontaneous polarization field to separate photogenerated carriers, resulting in a self-driven UV photoelectric detection. Till now, significant progress has been made on BTO-based self-driven photodetectors, however, the reported devices tended to exhibit low responsivity (10^{-8}–10^{-7} A·W^{-1}) except the use of high-quality single crystalline materials. In this work, we have fabricated a high-performance NiO/BTO/ITO p-i-n heterojunction structure self-driven UV photodetector using a low-cost RF sputtering technique. By coupling the ferroelectric depolarization field of BTO with the built-in field of p-i-n junction, the separation and migration of photogenerated carriers can be greatly promoted. Therefore, the responsivity at 255 nm of our device can reach to 3.4×10^{-5} A·W^{-1} under the poling-up state, which is much higher than that of reported UV photodetectors prepared from amorphous and ceramic BTO. In addition, our device exhibits a fast response speed of 0.3 s/0.4 s. The findings in this work provide a new strategy for improving the performance of BTO-based photodetectors.

Key words: $BaTiO_3$; ferroelectric effect; self-driven; UV photodetector; p-i-n junction; depolarization field
CLC number: TN23; O482.31 **Document code**: A **DOI**: 10.37188/CJL.20240118

铁电效应调控的高性能 p-NiO/i-$BaTiO_3$/n-ITO 自供能紫外光电探测器

洪涵真[1,2], 刘可为[1,2*], 杨佳霖[1], 陈 星[1,2], 朱勇学[1], 程 祯[1], 李炳辉[1], 刘 雷[1,2], 申德振[1,2]

(1. 中国科学院长春光学精密机械与物理研究所 发光学及应用国家重点实验室, 吉林 长春 130033;
2. 中国科学院大学 材料科学与光电工程研究中心, 北京 100049)

摘要: 近年来,自供能的紫外光电探测器由于无需任何外部偏压即可工作而成为军事和民用领域的研究热点。其中,钛酸钡(BTO)作为一种宽禁带铁电材料,拥有良好的铁电、压电和热电性能,可以产生本征自发极

收稿日期: 2024-04-28; **修订日期**: 2024-05-09
基金项目: 国家自然科学基金(62074148, 61875194, 12204474, 11727902, 12304111, 12304112); 中组部万人计划青年拔尖项目; 中国科学院青年创新促进会(2020225); 吉林省自然科学基金(20220101053JC); 吉林省中青年科技创新创业卓越人才(团队)项目(20220508153RC); 寒地建筑综合节能教育部重点实验室开放课题(JLJZHDKF022020007)
Supported by National Natural Science Foundation of China(62074148, 61875194, 12204474, 11727902, 12304111, 12304112); The National Ten Thousand Talent Program for Young Top-notch Talents; Youth Innovation Promotion Association, CAS (2020225); Jilin Province Science Fund(20220101053JC); Jilin Province Young and Middle-Aged Science and Technology Innovation Leaders and Team Project(20220508153RC); The Foundation of Key Laboratory of Architectural Cold Climate Energy Management, Ministry of Education(JLJZHDKF022020007)

化场来分离光生载流子,从而实现自供能紫外光电探测。到目前为止,基于BTO的自供能光电探测器已经取得了巨大进展,然而,除了使用高质量的单晶材料外,所报道的器件往往表现出低响应度(10^{-8}~10^{-7} A·W^{-1})。本文利用低成本的射频溅射技术,制造了一种高性能的NiO/BTO/ITO p-i-n异质结构自供能紫外光电探测器。通过将BTO的铁电去极化场和p-i-n结的内建电场耦合,能有效提高光生载流子的分离和迁移。因此,该器件在正极化态下255 nm波长紫外光照射下的响应度可以达到3.4×10^{-5} A·W^{-1},远远高于其他已报道的基于非晶态和陶瓷BTO制备的紫外光电探测器。此外,该器件具有0.3 s/0.4 s的快速响应时间。本工作为提高BTO光电探测器的性能提供了一种新的策略。

关 键 词:钛酸钡;铁电极化;自供能;紫外光电探测器;p-i-n结;去极化场

1 Introduction

In 1920, Valasek[1], a French scientist, discovered Rochelle salt (potassium sodium tartrate, NaKCHO·4H_2O) and proposed the concept of "ferroelectricity" which is defined as a nonlinear dielectric behavior under an electric field. In ferroelectric materials, under normal conditions, electric dipole moments form between positive and negative charge centers in a unit cell, resulting in spontaneous polarization without applying any electric field[2]. Therefore, ferroelectric materials are diversely applied in memory devices[3-5], actuators[6-7], sensors[8], energy storage[9] and photocatalysis[10-12]. In recent years, self-driven UV photodetectors have received extensive attention in both military and civilian fields because they can work without any external bias[13-16]. Among various ferroelectric materials, Barium titanate ($BaTiO_3$, abbreviated as BTO) has a typical perovskite structure with a bandgap of ~3.2-4.6 eV, and thus it is very suitable for UV detection. In addition, as an environmentally friendly ferroelectric material, BTO possesses good ferroelectric, piezoelectric, and pyroelectric properties, which could generate intrinsic spontaneous polarization fields to separate photogenerated carriers, resulting in a self-driven photoelectric detection[17-20]. Till now, although BTO self-driven photodetectors have made significant progress, the reported devices tended to exhibit low responsivity (10^{-8}-10^{-7} A·W^{-1}) in addition to the use of expensive high-quality single crystal materials[21-22]. Although combining the photovoltaic effect with ferroelectric, piezoelectric or pyroelectric effects can improve the responsivity of the BTO-based devices, it is still significantly lower than that of traditional semiconductor self-driven detectors[23-24].

More recently, our group have achieved a high-performance self-driven photodetector by constructing an amorphous-$BaTiO_3$/p-Si ferroelectric-semiconductor heterojunction by coupling the ferroelectric depolarization electric field and built-in electric field at the heterojunction interface, and the responsivities of the device could reach up to 0.027 A·W^{-1} at 365 nm[25]. However, due to the presence of a narrow bandgap of Si, this device has a strong response to visible light, so it is not suitable for intrinsic UV detection. Here, we have designed and fabricated a NiO/BTO/ITO p-i-n heterojunction structure self-driven UV photodetector using a low-cost radio-frequency(RF) sputtering technique. The combination of a ferroelectric depolarization field (E_{dp}) with the p-i-n built-in field ($E_{built\text{-}in}$) could enhance the separation and migration of photogenerated carriers. When the depolarization field of $BaTiO_3$ is in the same direction as the built-in electric field of the p-i-n junction (poling-up state), the responsivity is improved to 3.4×10^{-5} A·W^{-1}, which is significantly higher than that of reported photodetectors prepared from amorphous and ceramic BTO.

2 Experiment

2.1 Fabrication of Heterojunction Photodetector

ITO, BTO and NiO films were successively deposited onto c-Al_2O_3 substrate by RF magnetron sputtering method. Firstly, 50-nm-thick ITO film was sputtered with a sputtering power of 100 W in an atmosphere of Ar and O_2 gas mixture (Ar∶O_2 = 5∶1) with a pressure of 1.2 Pa. The as-grown ITO film was then annealed at 750 ℃ for 1 hour in O_2 atmosphere

in a tube furnace to increase crystal quality and to improve conductivity.

After that, 200-nm-thick BTO film was grown on ITO at a temperature of 290 ℃ in pure Ar gas atmosphere (0.8 Pa) with a sputtering power of 80 W. Then, the NiO film with a thickness of 50 nm was prepared on BTO at room temperature, and a mixture of Ar and O_2 gas (Ar∶O_2 = 2∶1) was selected as the sputtering gas with a pressure of 0.8 Pa and a sputtering power of 150 W.

Finally, gold (Au) and indium (In) are chosen as the Ohmic contact electrodes with NiO and ITO layers, respectively, which are deposited by DC magnetron sputtering technology using a shadow mask.

2.2 Characterizations

The crystal structure was characterized using X-ray diffraction (XRD) (Bruker D8GADDS, Cu Kα radiation, λ = 0.154 1 nm). Scanning electron microscope (SEM) (HITACHI S-4800, the mode of measurement: secondary electrons) was used to evaluate the surface morphology and cross-sectional morphology of the sample. Optical properties were characterized by a UV3101 (PC) scanning spectrophotometer technique. The current-voltage (I-V) curves and photo response characteristics of the photodetector were tested by an Agilent B1500A semiconductor device analyzer. The electrical properties of n-ITO and p-NiO films were investigated by the Lakeshore 7707 Hall measurement system. All the measurements were performed at room temperature.

3 Results and Discussion

As shown in Fig. 1(a), the NiO/BTO/ITO p-i-n heterojunction structure was fabricated by sputtering n-type ITO, intrinsic BTO and p-type NiO onto c-Al_2O_3 in sequence. Au and In Ohmic contact electrodes were prepared on p-NiO and n-ITO surfaces, respectively. Hall measurement results illustrated that the NiO film exhibits p-type conductivity. Its carrier concentration was found to be 3.8×10^{19} cm^{-3} with a Hall mobility of 0.37 $cm^2\cdot V^{-1}\cdot s^{-1}$. Meanwhile, ITO film shows typical n-type conductivity with a carrier concentration of 1.8×10^{20} cm^{-3} and a mobility of 2.1 $cm^2\cdot V^{-1}\cdot s^{-1}$. A cross-sectional SEM image of the NiO/BTO/ITO p-i-n heterojunction was presented in Fig. 1(b). And the thicknesses of NiO, BTO and ITO layers have been estimated to be 50 nm, 200 nm and 50 nm, respectively.

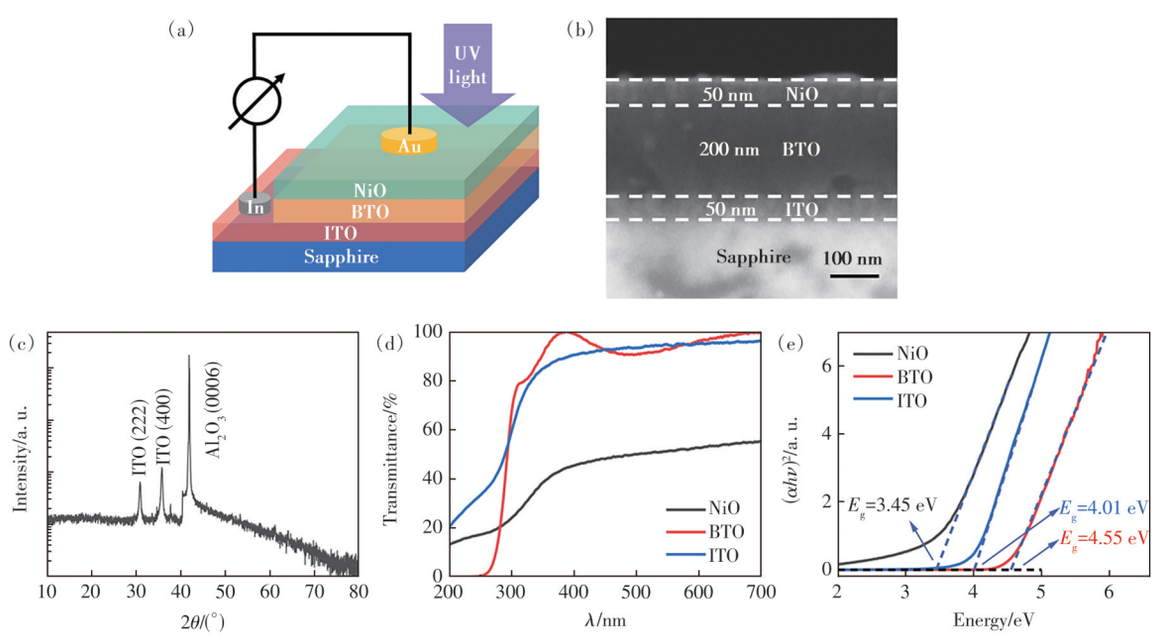

Fig.1 (a) Schematic of the self-driven UV photodetector. (b) Cross-sectional SEM image of the device. (c) XRD pattern of NiO/BTO/ITO p-i-n heterojunction. Transmission spectra (d) and Tauc plots (e) of NiO, BTO and ITO films

In Fig. 1(c), XRD patterns have been acquired to determine the crystal structure of NiO/BTO/ITO p-i-n heterojunction on c-Al_2O_3 substrate. A strong (0006) diffraction peak of c-Al_2O_3 is at around 2θ =

41.68°. In addition, two peaks at 2θ = 30.8° and 35.7° can be clearly observed, corresponding to (222) and (400) diffraction peaks of BCC ITO, respectively (JCPDS No. 44-1087)[26-28]. Moreover, the diffraction patterns of NiO and BTO are absent, indicating that they are both fully amorphous. Due to the presence of small, ordered clusters within the amorphous network, ferroelectricity is exhibited in amorphous BTO, although with a remnant polarization lower than that observed in crystals[29].

Fig. 1(d) represents the transmission spectra of each film on sapphire substrates. Clearly, both BTO and ITO films exhibited high transparency of over 90% in the visible region, while only ~50% transmittance in the range of 400−700 nm can be observed for NiO. Moreover, the band gaps of NiO, ITO and BTO thin films were estimated to be 3.45 eV, 4.01 eV and 4.55 eV using the Tauc plot method in Fig. 1(e), respectively. It is worth noting that the band gap of amorphous films (4.2−4.6 eV)[30] is higher than that of the crystalline films and bulk single crystals (~3.2 eV)[31].

To facilitate the creation of Ohmic contacts, we opted for indium with low work function (4.12 eV) as the electrode for the n-ITO layer and gold with high work function (5.1 eV) for the p-NiO layer[32]. Fig. 2(a) shows the *I-V* characteristic curves of Au/p-NiO/Au and In/n-ITO/In under dark condition. The linearity of *I-V* characteristics suggested the formation of excellent Ohmic contacts both between Au and p-NiO and between In and n-ITO. Therefore, only the built-in electric field generated at the p-i-n heterojunction interface and the ferroelectric depolarization field in BTO can be responsible for separating the photogenerated e^--h^+ pairs and helping produce the rectifying behavior. As shown in Fig. 2(b), the *I-V* curve of the NiO/BTO/ITO p-i-n heterojunction in dark condition shows an obvious rectifying behavior.

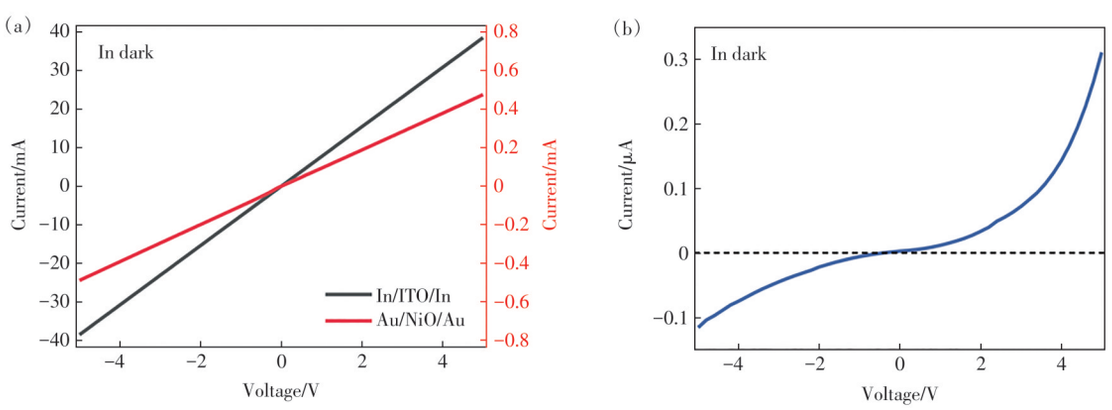

Fig.2 *I-V* curves of Au/p-NiO/Au and In/n-ITO/In(a), and NiO/BTO/ITO p-i-n heterojunction(b) in dark

Given that the Curie point of BTO is ~120 ℃[33-34], the device was heated at 150 ℃ for 5 min to attain an unpolarized state. After applying +10 V and −10 V bias to the device for 200 s, the poling-up and poling-down states can be achieved in the p-i-n photodetector, respectively (Fig. 3(a)). In the poling-up state, the depolarization field (E_{dp}) in $BaTiO_3$ is consistent with the built-in electric field of the p-i-n junction ($E_{built\text{-}in}$) in direction, and thus the overall electric field is intensified. Conversely, when the depolarization field is opposite in direction to the built-in electric field, that is, the poling-down state, the total electric field is weakened.

The photocurrent response properties of the device were investigated by periodically switching the 255 nm light (2.33 mW·cm^{-2}) ON and OFF at 0 V under different polarization states as shown in Fig. 3(b). And the result indicates that the device exhibits robust and consistent photoresponse to intermittent illumination, characterized by its rapid and stable behavior. When the device is in the poling-up state, the $E_{built\text{-}in}$ is in the same direction as the E_{dp}, thus increasing the photocurrent from 7.6 nA to 8.9 nA. In contrast, when the device is in the poling-down state, the $E_{built\text{-}in}$ and E_{dp} are in opposite directions, and a significant drop in photocurrent can be

observed from 7.6 nA to 4.2 nA. As a result, the photoelectric response of the p-i-n heterojunction device can be effectively adjusted by an external voltage. In particular, the responsivity is calculated to be 3.4×10^{-5} A·W^{-1} for the device in poling-up state with a sensitive area of 0.112 cm^2. Additionally, 10%－90% rise and 90%－10% decay time of the p-NiO/i-BTO/n-ITO device in poling-up state are estimated to be 0.3 s and 0.4 s, respectively. The effect of polarization state on response speed is not significant (Fig. 3(c)), however, the introduction of polarization slightly decreases the rise time, which may be related to the E_{dp} accelerating the separation of charge carriers. The wavelength-dependent responsivity of the device in three states is shown in Fig. 3(d) from 255 nm to 660 nm. It has been shown that the device does not respond to visible light and achieves maximum responsivity at the wavelength of 255 nm. It's worth noticing that, despite the fact that both NiO and ITO possess relatively narrow bandgaps, the photoresponse is mainly located in solar blind area. This may be because the response can be largely attributed to the BTO layer, which exhibits a high absorption rate of ultraviolet radiation. Consequently, within the structure of the device, BTO acts as the fundamental photosensitive layer, while NiO and ITO primally establish the internal electric field and supply charge carriers.

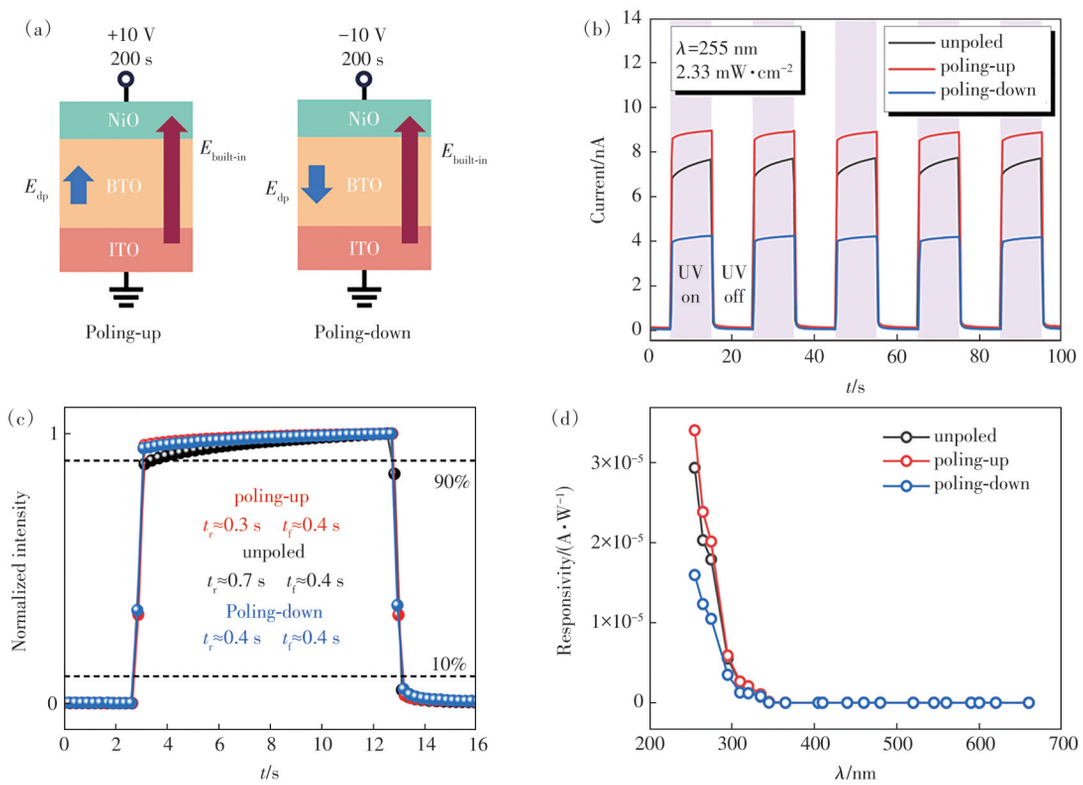

Fig.3　(a) Schematic of the p-i-n heterojunction device in poling up and poling down states. Photocurrent responses (b), rise time and fall time in one cycle (c) and response spectra (d) of the photodetector at 0 V bias in various polarization states

Tab. 1 provides a comparative summary of the responsivity and rise/fall time of the self-driven photodetector developed in this study with the reported devices utilizing BTO ferroelectric materials. The p-NiO/i-BTO/n-ITO device presented in this work exhibits a superb self-driven photodetection performance. To the best of our knowledge, this device is superior in responsivity (3.4×10^{-5} A·W^{-1}) to the other reported BTO-based self-driven UV photodetectors due to the efficient combination of the depolarization field in BTO and the built-in electric field in the p-i-n heterojunction. And the response speed of our device is also faster than or comparable to the reported results. Additionally, the fabrication process of the present p-NiO/i-BTO/n-ITO device is advantageous due to its low-cost and suitability for large-scale production.

Tab. 1 Comparison of the key parameters of our device and other $BaTiO_3$-based self-driven photodetectors reported previously

Device structure	Wavelength/nm	t_r/t_f/s	Responsivity/($A \cdot W^{-1}$)	Ref.
ITO/BTO/Ag	365	0.57/31.8	2.4×10^{-8}	[35]
Ag/BTO/Ag	365	0.5/23	0.48×10^{-8}	[36]
ITO/BTO/Ag	405	0.4/1.6	$<3.5\times10^{-7}$	[24]
ITO/BTO/ITO	365	0.5/0.2	2.3×10^{-7}	[37]
ITO/BTO/Ag	365	0.6/0.5	$\sim10^{-7}$	[22]
Ag/BTO/Ag	365	0.65/13.44	$\sim10^{-7}$	[21]
NiO/BTO/ITO	255	0.3/0.4	3.4×10^{-5}	This work

4 Conclusion

In summary, a high-performance self-driven p-NiO/i-BTO/n-ITO UV photodetector was fabricated by a low-cost RF sputtering method. It is demonstrated that the device could enhance the separation and migration of the photogenerated carriers through the combination of the E_{dp} of BTO with the $E_{built\text{-}in}$ of the p-i-n junction, thus exhibiting higher photocurrent. As a result, we have successfully achieved a high responsivity of 3.4×10^{-5} $A \cdot W^{-1}$ at 255 nm under 0 V bias, which is significantly higher than that of other reported self-driven photodetectors based on amorphous and ceramic BTO. Additionally, our device exhibits a very fast response speed with rise and fall time of 0.3 s and 0.4 s, respectively. Our device structure and design concept provide a simple and feasible way for realizing high-performance self-powered photodetectors.

Response Letter is available for this paper at: http://cjl.lightpublishing.cn/thesisDetails#10.37188/CJL.20240118.

References:

[1] VALASEK J. Piezo-electric and allied phenomena in Rochelle salt [J]. *Phys. Rev.*, 1921, 17(4): 475-481.

[2] WU M H. 100 years of ferroelectricity [J]. *Nat. Rev. Phys.*, 2021, 3(11): 726.

[3] ZULEEG R, WIEDER H H. Effect of ferroelectric polarization on insulated-gate thin-film transistor parameters [J]. *Solid-State Electron.*, 1966, 9(6): 657-661.

[4] MA T P, HAN J P. Why is nonvolatile ferroelectric memory field-effect transistor still elusive? [J]. *IEEE Electron Dev. Lett.*, 2002, 23(7): 386-388.

[5] MARTIN L W, RAPPE A M. Thin-film ferroelectric materials and their applications [J]. *Nat. Rev. Mater.*, 2017, 2(2): 16087.

[6] SCHROEDER U, PARK M H, MIKOLAJICK T, *et al*. The fundamentals and applications of ferroelectric HfO_2 [J]. *Nat. Rev. Mater.*, 2022, 7(8): 653-669.

[7] NEWNS D M, ELMEGREEN B G, LIU X H, *et al*. The piezoelectronic transistor: a nanoactuator-based post-CMOS digital switch with high speed and low power [J]. *MRS Bull.*, 2012, 37(11): 1071-1076.

[8] SETTER N, DAMJANOVIC D, ENG L, *et al*. Ferroelectric thin films: review of materials, properties, and applications [J]. *J. Appl. Phys.*, 2006, 100(5): 051606.

[9] BHATIA B, DAMODARAN A R, CHO H, *et al*. High-frequency thermal-electrical cycles for pyroelectric energy conversion [J]. *J. Appl. Phys.*, 2014, 116(19): 194509.

[10] LIU L Z, WANG S B, HUANG H W, *et al*. Surface sites engineering on semiconductors to boost photocatalytic CO_2 reduction [J]. *Nano Energy*, 2020, 75: 104959.

[11] FU J W, YU J G, JIANG C J, *et al*. G-C_3N_4-based heterostructured photocatalysts [J]. *Adv. Energy Mater.*, 2018, 8(3): 1701503.

[12] HU C, TU S G, TIAN N, *et al*. Photocatalysis enhanced by external fields [J]. *Angew. Chem. Int. Ed.*, 2021, 60(30): 16309-16328.

[13] ASHTAR M, YANG J X, YANG Y, *et al*. Improved photodetection performance of self-powered UV photodetector based

on PZT/CuSCN heterojunction [J]. *Sol. Energy Mater. Sol. Cells*, 2024, 270: 112812.

[14] CHENG Y Y, MAO J X, ZHU H Y, *et al*. Ferroelectric enhanced Ga_2O_3/BFMO-based deep ultraviolet photovoltaic detectors with dual electric fields for photogenerated carrier separation [J]. *J. Mater. Chem.* C, 2023, 11(43): 15197-15204.

[15] HAN Z K, LUO B C, WANG S H, *et al*. Ferroelectrically modulated and enhanced photoresponse of a Ag/PZT/NSTO self-powered photodetector in the ultraviolet range [J]. *J. Mater. Chem.* C, 2024, 12(10): 3708-3714.

[16] YAN S, YANG G C, HE H F, *et al*. High-performance self-driven solar-blind ultraviolet photodetectors based on $HfZrO_2$/β-Ga_2O_3 heterojunctions [J]. *ACS Appl. Mater. Interfaces*, 2023, 15(18): 22263-22273.

[17] DONG M J, ZHENG X M, LI Q, *et al*. Multi-effect coupling enhanced self-powered heterojunction ultraviolet photodetector with ultra-low detection limit [J]. *Mater. Today*, 2024, 74: 85-93.

[18] WOLDU T, RANEESH B, SREEKANTH P, *et al*. Size dependent nonlinear optical absorption in $BaTiO_3$ nanoparticles [J]. *Chem. Phys. Lett.*, 2015, 625: 58-63.

[19] CHEN L, LI H M, WU Z, *et al*. Enhancement of pyroelectric catalysis of ferroelectric $BaTiO_3$ crystal: the action mechanism of electric poling [J]. *Ceram. Int.*, 2020, 46(10): 16763-16769.

[20] ACOSTA M, NOVAK N, ROJAS V, *et al*. $BaTiO_3$-based piezoelectrics: fundamentals, current status, and perspectives [J]. *Appl. Phys. Rev.*, 2017, 4(4): 041305.

[21] MA N, YANG Y. Boosted photocurrent in ferroelectric $BaTiO_3$ materials *via* two dimensional planar-structured contact configurations [J]. *Nano Energy*, 2018, 50: 417-424.

[22] SONG K, MA N, MISHRA Y K, *et al*. Achieving light-induced ultrahigh pyroelectric charge density toward self-powered UV light detection [J]. *Adv. Electron. Mater.*, 2019, 5(1): 1800413.

[23] QIAN W Q, WU H T, YANG Y. Ferroelectric $BaTiO_3$ based multi-effects coupled materials and devices [J]. *Adv. Electron. Mater.*, 2022, 8(10): 2200190.

[24] MA N, ZHANG K W, YANG Y. Photovoltaic-pyroelectric coupled effect induced electricity for self-powered photodetector system [J]. *Adv. Mater.*, 2017, 29(46): 1703694.

[25] HAN W S, LIU K W, YANG J L, *et al*. High-performance self-powered amorphous-$BaTiO_3$/p-Si heterojunction photodetector controlled by ferroelectric effect [J]. *Appl. Surf. Sci.*, 2023, 615: 156371.

[26] SHIH G H, ALLEN C G, POTTER B G JR. RF-sputtered Ge-ITO nanocomposite thin films for photovoltaic applications [J]. *Sol. Energy Mater. Sol. Cells*, 2010, 94(5): 797-802.

[27] YAN Y F, ZHOU J, WU X Z, *et al*. Structural instability of Sn-doped In_2O_3 thin films during thermal annealing at low temperature [J]. *Thin Solid Films*, 2007, 515(17): 6686-6690.

[28] WAN N, WANG T, SUN H C, *et al*. Indium tin oxide thin films for silicon-based electro-luminescence devices prepared by electron beam evaporation method [J]. *J. Non-Cryst. Solids*, 2010, 356(18-19): 911-916.

[29] MACKENZIE J D, XU Y H. Ferroelectric materials by the sol-gel method [J]. J. *Sol-Gel Sci. Technol.*, 1997, 8(1): 673-679.

[30] LIU W T, LAKSHMIKUMAR S T, KNORR D B, *et al*. Deposition of amorphous $BaTiO_3$ optical films at low temperature [J]. *Appl. Phys. Lett.*, 1993, 63(5): 574-576.

[31] MENG K, LI W H, TANG X G, *et al*. A review of a good binary ferroelectric ceramic: $BaTiO_3$-$BiFeO_3$ [J]. *ACS Appl. Electron. Mater.*, 2022, 4(5): 2109-2145.

[32] MENG J P, LEE C, LI Z. Adjustment methods of Schottky barrier height in one- and two-dimensional semiconductor devices [J]. *Sci. Bull.*, 2024, 69(9): 1342-1352.

[33] LIU J, SU L, ZHANG X L, *et al*. Ferroelectric-optoelectronic hybrid system for photodetection [J]. *Small Methods*, 2024, 8(2): 2300319.

[34] LI H Y, BOWEN C R, YANG Y. Scavenging energy sources using ferroelectric materials [J]. *Adv. Funct. Mater.*, 2021, 31(25): 2100905.

[35] JI Y, WANG Y H, YANG Y. Photovoltaic-pyroelectric-piezoelectric coupled effect induced electricity for self-powered coupled sensing [J]. *Adv. Electron. Mater.*, 2019, 5(6): 1900195.

[36] MA N, YANG Y. Enhanced self-powered UV photoresponse of ferroelectric $BaTiO_3$ materials by pyroelectric effect [J]. *Nano Energy*, 2017, 40: 352-359.

[37] ZHAO K, OUYANG B S, YANG Y. Enhancing photocurrent of radially polarized ferroelectric $BaTiO_3$ materials by ferro-pyro-phototronic effect [J]. *iScience*, 2018, 3: 208-216.

洪涵真(1998-),女,浙江杭州人,硕士研究生,2021年于南京航空航天大学获得学士学位,主要从事宽禁带半导体光电材料与器件的研究。

E-mail: honghanzhen21@mails. ucas. ac. cn

刘可为(1981-),男,辽宁铁岭人,博士,研究员,博士生导师,2008年于中国科学院长春光学精密机械与物理研究所获得博士学位,主要从事宽禁带半导体光电材料与器件方面的研究。

E-mail: liukw@ciomp. ac. cn